Ionics (2019) 25:3387–3396
https://doi.org/10.1007/s11581-019-02886-w

ORIGINAL PAPER

$(SiO_2)_{100-x}$-Ni_x ($x = 2.5, 10.0$) Composite-based photoanode with polymer gel electrolyte for increased dye-sensitized solar cell performance

Huda Abdullah[1] · Mohammad Khairusani Zainudin[1] · Masrianis Ahmad[1] · Savisha Mahalingam[2] · Abreeza Manap[2]

Received: 29 July 2018 / Revised: 30 December 2018 / Accepted: 20 January 2019 / Published online: 1 February 2019

Abstract

This work aims on the degradation performance of $(SiO_2)_{100-x}$-Ni_x ($x = 2.5, 10.0$) photoanodes incorporating with liquid and gel polymer electrolyte for dye-sensitized solar cell (DSSC). The silica doped with nickel and gel polymer electrolyte was prepared by sol-gel polymerization of tetraethyl orthosilicate and sol-gel polymerization of polyacrylonitrile (PAN), respectively. The utilization of PAN-based gel polymer electrolyte improved the value of open circuit voltage due to its high ionic conductivity and mechanical stability in DSSC. The $(SiO_2)_{90.0}$-$Ni_{10.0}$-based DSSC utilizing PAN-based gel polymer electrolyte exhibited the highest power conversion efficiency of 2.96%. The field emission electron microscopy images show larger average particle size with greater porosity in the $(SiO_2)_{90.0}$-$Ni_{10.0}$ thin film. Moreover, the Brunauer-Emmett-Teller analysis determines greater active surface area on $(SiO_2)_{90.0}$-$Ni_{10.0}$ thin films that indicates more dye molecules may adsorb on the mesoporous photoanode to facilitate electron transport in the DSSC.

Keywords Dye-sensitized solar cells (DSSCs) · Sol-gel · Gel polymer electrolyte · Silica · Nickel

Introduction

Fossil fuels are used as the main energy source for centuries to meet the economic needs. However, the uses of fossil fuels greatly contribute to the increase of greenhouse gas emissions such as carbon dioxide that leads to severe climate change and global warming [1]. In order to address this issue, we need to use an alternate clean renewable energy source to power things up. Power from the sun is an effective renewable energy source that does not emit dangerous greenhouse gases.

Highlights
- A novel silica incorporated with nickel-based hybrid photoanode was prepared by sol-gel process for dye-sensitized solar cell (DSSC)
- Polyacrylonitrile (PAN)-based polymer gel electrolyte prepared by modified sol-gel process was used to increase the lifetime of the DSSC
- Higher doping of nickel enhanced the ionic conductivity and subsequently increased the solar power conversion efficiency of the DSSC

✉ Huda Abdullah
huda.abdullah@ukm.edu.my

[1] Department of Electrical, Electronic and System Engineering, Faculty of Engineering and Built Environment, Universiti Kebangsaan Malaysia, 43600 Bangi, Selangor, Malaysia

[2] Institute of Sustainable Energy, Universiti Tenaga Nasional, Jalan IKRAM-UNITEN, 43000 Kajang, Selangor, Malaysia

Within the last decade, several studies on solar energy that can be converted into electricity by using the theory of photovoltaic (PV) effect have been carried out [2]. The third generation PV cells are the dye-sensitized solar cells (DSSCs) that were introduced by O'Regan and Grätzel in 1991 [3]. DSSCs are more desirable than the other generation of PV cells due to their low-cost fabrication, simple manufacturing process, and high PV efficiency [4]. DSSCs consist of three layers of sandwiched structure: (1) photoanode; (2) counter electrode; and (3) electrolyte [5].

Although the conventional metal oxide semiconductor (TiO_2) acting as the photoanode layer achieved high PV efficiency around 15%, it has a drawback of high electron recombination rate that degrades the performance of the DSSC [6]. Thus, various types promising alternative photoanodes have been extensively studied such as ZnO [7], SnO_2 [8], and In_2O_3 [9]. The wide band gap material of silicone dioxide (SiO_2) with energy band gap of 3.25 eV has great potential as photoanode layer in DSSCs because it is low-cost and environmentally friendly [10]. According to Shin et al. [11], SiO_2 is capable of reducing the electron recombination rate in DSSCs. Besides that, SiO_2 also has a large surface area that promotes dye absorption [10]. However, the SiO_2-based DSSCs still show lower power conversion efficiency. Therefore, Li et al. [12] mentioned that incorporation of

transition metal such as nickel (Ni) in the photoanode may increase the ionic conductivity and subsequently increase the solar power conversion efficiency of DSSCs.

Furthermore, silica (SiO_2) is the most extensively studied type of compound because of their low bulk density, hydrophobicity, great surface area, and optical transparency [11]. Silicon alkoxides are the most common type of family precursors for sol-gel silica processing [11]. The most common family of precursors for sol-gel silica processing are silicon alkoxides (alkoxysilanes). Tetraethyl orthosilicate (TEOS) is the first alkoxide of the series [10]. As TEOS is reactive enough to form gel networks with other materials, we used Ni and synthesized silica composites in this work for enhanced light-harvesting properties for DSSC [12]. The silica was prepared by sol-gel polymerization of TEOS under hydrolytic condition using base catalyst (ammonia solution, NH_3).

The silica was prepared by sol-gel polymerization of TEOS (Si $(OC_2H_5)_4$) involving hydrolysis and condensation reactions and followed by special drying process. Silanols (Si-OH) and ethanol (EtOH or C_2H_5OH) are formed during hydrolysis reaction when TEOS and water (H_2O) are mixed together [10]. The condensation process occurs between two Si-OH groups to form binding oxygen or a siloxane group (Si-O-Si) [10]. The equation scheme of the hydrolysis and condensation process is shown in Fig. 1.

Moreover, the conventional ionic liquid electrolyte used in DSSCs causes mass-transport limitation problems due to high viscosity [13]. Hence, liquid electrolyte strongly affects the overall conversion efficiency. In order to improve the charge transfer of the electrolyte, PAN-based gel polymer was employed in this present work as catalyst. PAN-based gel polymer exhibits high conductivities that lead to greater electron lifetime and improved power conversion efficiency [14, 15]. PAN-based gel polymer (PAN:EC:PC:$Pr_4N^+I^-$:I_2) consists a mixture of PAN, ethylene carbonate (EC), propylene carbonate (PC), tetrapropylammonium iodide ($Pr_4N^+I^-$) salt, and iodine (I_2).

Furthermore, larger cation of Pr_4N^+ gives a high open-circuit voltage (V_{oc}) but low short-circuit current density (J_{sc}) [16]. Their large size and lower charge density makes them not to intercalate into the metal oxide or get attached to the metal oxide surface easily and therefore shows no effect on the conduction band edge of the metal oxide [17]. Hence, larger cations do not influence the electron injection and give low J_{sc} values. Thus, in this work, we have replaced $Pr_4N^+I^-$ with potassium iodide (KI) which is a smaller cation for greater J_{sc} and V_{oc} to obtain modified PAN-based gel polymer electrolyte in the form of PAN:EC:PC:KI:I_2. Smaller cations have high charge density that can intercalate in the metal oxide and improve photo-generated electron injection and increase the photocurrent and J_{sc}.

This is the first work conducted on two different amounts of Ni doping (2.5%, 10.0%) in silica-based photoanode nanocomposite utilizing PAN-based gel polymer electrolyte. The objective of this study is to determine the photovoltaic performance of $(SiO_2)_{100-x}$-Ni_x ($x = 2.5$, 10.0) with the conventional liquid electrolyte and PAN-based gel electrolyte. This work gains its novelty in the preparation method of silica doped with nickel and modified PAN-based gel polymer electrolyte by novel sol-gel method. Nickel doping of 2.5% and 10% were used because Ahmad et al. [18] mentioned that optimum amount of nickel doped in SiO_2-based DSSC is in the range of 2.5–10%. Besides that, in order to produce a homogeneous SiO_2-Ni nanocomposite powder, a preferable amount of nickel doped is between 2.5 and 10%.

The efficiency of a state-of-the-art DSSC is 13% in 2014 using volatile solvent-based electrolytes [19]. However, there are some limitations such as electrolyte encapsulation, leakage, and cell deterioration. Even though the obtained current results have lower efficiency than the efficiency of a state-of-

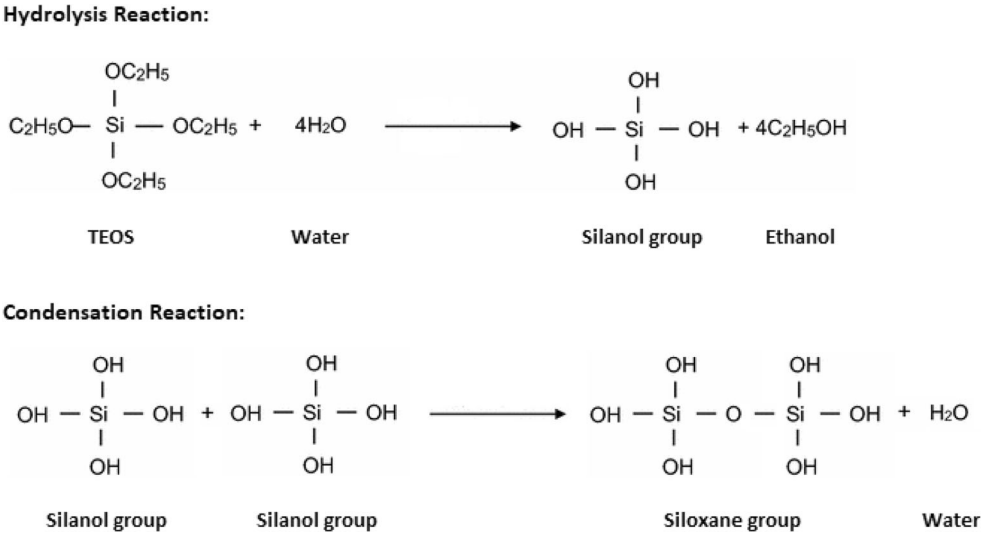

Fig. 1 Equation scheme of the hydrolysis and condensation process of sol-gel polymerization of TEOS

the-art DSSC, this work contributes to the practical industrial application by using this kind of gel electrolyte. Compared with the commercial electrolyte Solaronix MPN-100, this unique gel electrolyte enhances the J_{sc} and the power conversion efficiency. The objective is supported by structural and morphology analysis of $(SiO_2)_{100-x}$-Ni_x ($x = 2.5$, 10.0) by using X-ray diffractometer (XRD), Brunauer-Emmett-Teller (BET), and field emission electron microscopy (FESEM). The PV performance of DSSC was evaluated through photocurrent density-voltage (*J-V*) curve.

Experimental details

Materials

The chemicals used in this work are TEOS (Sigma-Aldrich), ethanol (EtOH) 95% (HmbG Chemicals), nickel (II) nitrate hexahydrate (R&M Chemicals), ammonia 25% (R&M Chemicals), diethanolamine (DEA) (Merck, Germany), ethylene carbonate 98% (Sigma-Aldrich), propylene carbonate, (R&M Chemicals), potassium iodide (R&M Chemicals), iodine 99.8% (Sigma-Aldrich), polyacrylonitrile PAN (Good Fellow), and iodolyte MPN 100 (Solaronix).

Preparation of silica and nickel composite network

Base-catalyzed hydrolysis occurs when an aqueous solution of TEOS (Si $(OEt)_4$) was added in the solvent of EtOH followed by continuous stirring for 1 h at 80 °C to form a clear solution before mixing deionized water (H_2O) and base ammonia (NH_3) solution (25% of weight/volume) as catalyst. The molar ratio of the TEOS:EtOH:H_2O mixture is 1:4:16. The mixture was then added into 30 mL of DEA mixed with drops (Ni_x ($x = 2.5$, 10.0)) of nickel (II) nitrate hexahydrate solution (Ni $(NO_3)_2 \cdot 6H_2O$). DEA acts as stabilizer to prevent agglomeration in the solution. The solution was then heated at 80 °C for overnight to complete the gelation process and form a slurry solution. The solution was filtered and rinsed with EtOH to remove the basicity caused by NH_3. The gelation was dried supercritically at 100 °C for 2 h to remove the excess solvent. Figure 2 shows the flowchart of preparing $(SiO_2)_{100-x}$-Ni_x ($x = 2.5$, 10.0) composite network. The hydrolysis and condensation process of sol-gel polymerization of TEOS, gelation process, and drying process is shown in Fig. 3.

Preparation of $(SiO_2)_{100-x}$-Ni_x ($x = 2.5$, 10.0) thin films

The thin films acting as photoanodes were prepared by depositing $(SiO_2)_{100-x}$-Ni_x ($x = 2.5$, 10.0) paste on clean fluorine-tin oxide (FTO) conducting substrates with an active surface area of 0.5 cm × 0.5 cm. $(SiO_2)_{100-x}$-Ni_x ($x = 2.5$, 10.0) was deposited on the conducting substrates by using a white glass rod known as doctor-blade technique. Then, the thin films were dried at 100 °C on a hot plate before annealing at 400 °C for 30 min. The thin films of $(SiO_2)_{100-x}$-Ni_x ($x = 2.5$, 10.0) were taken out of the furnace when the temperature dropped to 40 °C. Figure 3 shows the complete preparation of $(SiO_2)_{100-x}$-Ni_x ($x = 2.5$, 10.0) hybrid photoanode.

Preparation of gel polymer electrolyte by sol-gel polymerization of polyacrylonitrile

The gel polymer electrolyte (PAN:EC:PC:KI:I_2) was prepared in the ratio of 13:40:40:6:1. EC ($C_3H_4O_3$), PC ($C_4H_6O_3$), and KI were stirred on a hot plate at 60 °C for 1 h until the potassium iodide is fully dissolved. Then, the PAN is added into the mixture and stirred continuously at 110 °C for 5 min. Finally, I_2 is dropped carefully at room temperature and continuously stirred until a viscous gel-like solution is formed.

Fabrication of DSSC

The annealed thin films of $(SiO_2)_{100-x}$-Ni_x ($x = 2.5$, 10.0) were immersed in N719 dye for 24 h and rinsed with EtOH to remove the excess dye. Consequently, counter electrode was prepared by depositing platinum paste on a clean ITO substrate via screen printing technique. The platinum counter electrode was annealed at 450 °C for 60 min. The fabrication of DSSC took place by sandwiching the counter electrode and the annealed thin films of $(SiO_2)_{100-x}$-Ni_x ($x = 2.5$, 10.0). A layer of parafilm was used to attach the cell and binder clips to hold on both ends. The liquid electrolyte (Iodolyte MPN 100) and the lab-made PAN-based gel polymer electrolyte were injected individually into the sandwiched cell by forming an active area of 1 cm^2.

Characterization of the samples

The annealed thin films were characterized by means of XRD, BET, and FESEM. The fabricated DSSC was characterized to evaluate the performance of DSSC via the *J-V* curve. The structural characterization was done by using XRD (Siemens D-5000), CuKα radiation of 1.540 Å. The surface area was obtained through BET (Micromeritic ASAP 2020) analysis. The morphology of the annealed thin films was observed through FESEM (Zeisz Supra). The photovoltaic performance of the DSSCs was evaluated using the *J-V* curve measurement via linear sweep voltammetry unit (Gamry Physical Electrochemistry (PHE200)) under 100 mW/m^2 illumination (1.5 AM) of OSRAM halogen lamp, 50 W.

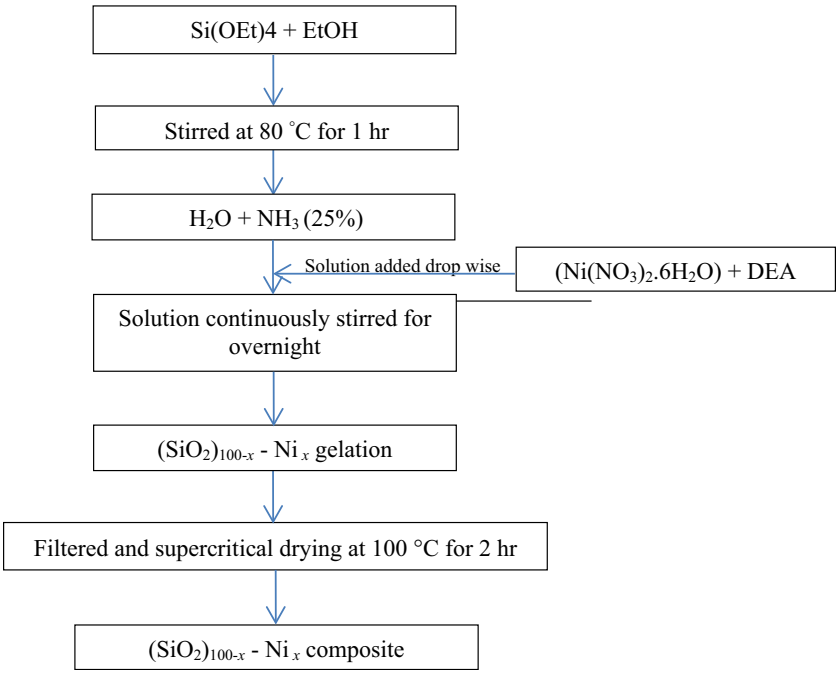

Fig. 2 Flowchart of preparation of $(SiO_2)_{100-x}$-Ni_x ($x = 2.5, 10.0$) composite

Result and discussion

XRD analysis

The XRD spectra of the thin films of $(SiO_2)_{100-x}$-Ni_x doped with Ni^{2+} of 2.5% and 10.0% are shown in the Fig. 4(a) and (b), respectively. Both the samples exhibited a broad peak at around 22° in the range of $2\theta = 15–35°$, corresponding to amorphous silica, and associated with low degree of crystallization of the silica support.

However, the $(SiO_2)_{97.5}$-$Ni_{2.5}$ shows narrow crystalline diffraction peaks of Ni and NiO. Diffraction peaks at 31.4°,

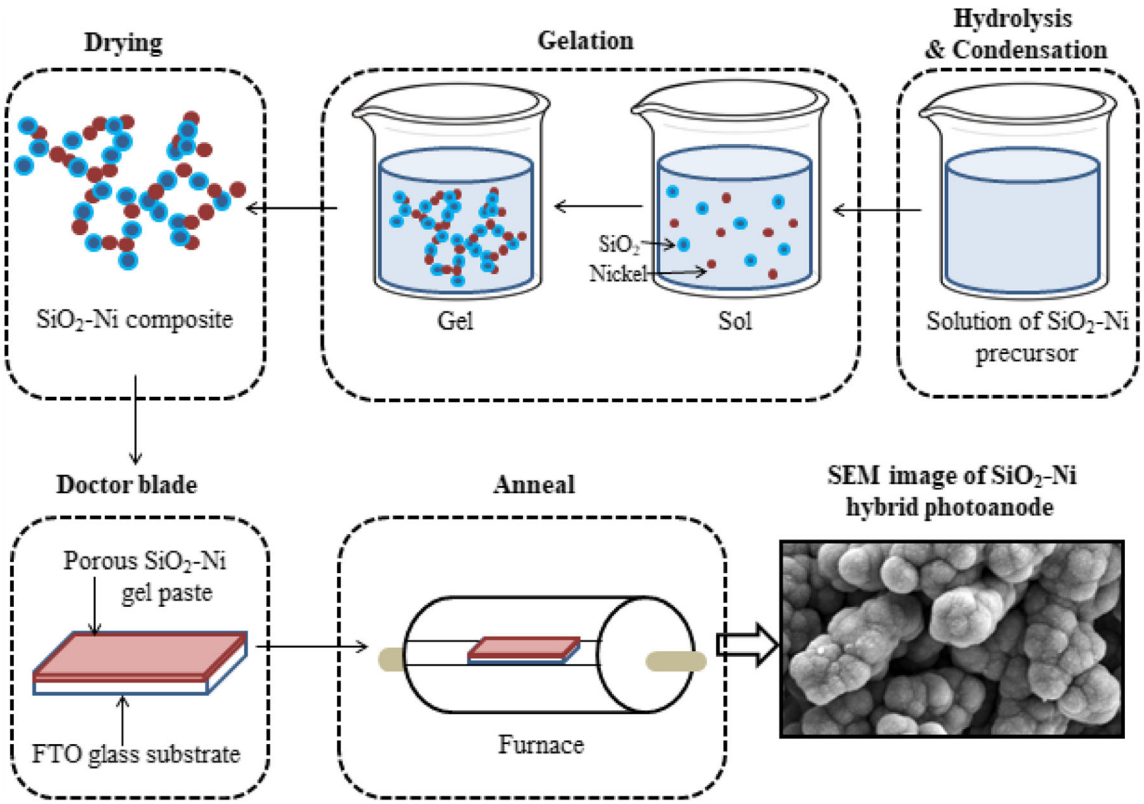

Fig. 3 Preparation of $(SiO_2)_{100-x}$-Ni_x ($x = 2.5, 10.0$) hybrid photoanode

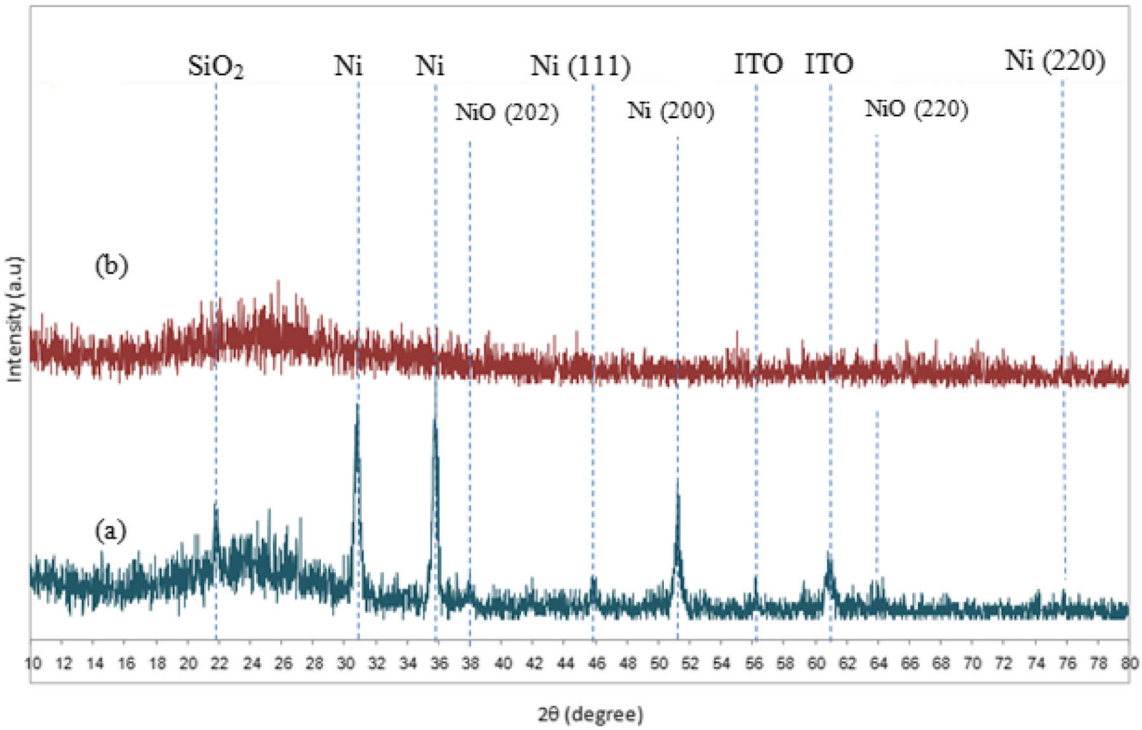

Fig. 4 XRD of $(SiO_2)_{100-x}$-Ni_x (a) $x = 2.5\%$ and (b) $x = 10.0\%$

45.5°, 51.81°, and 76° attributed to the hkl planes of (311), (111), (200), and (220) of Ni nanoparticles, respectively. The peaks located at 2θ of 36°, 38°, and 64° are related to (101), (202), and (220) indicating the presence of NiO crystals. Besides that, presence of ITO was also observed in the thin film of $(SiO_2)_{97.5}$-$Ni_{2.5}$. The result is in agreement with the observation over Ni-SiO_2 reported in the literature [18]. The presence of NiO nanoparticles indicates the formation of isolated NiO crystals which is seen in the FESEM image in Fig. 5 (a1). In addition, the narrow peaks of Ni and NiO show that the particle size of $(SiO_2)_{97.5}$-$Ni_{2.5}$ is large which is also in agreement with the FESEM image observed in Fig. 5 (a1).

No obvious diffraction peak of Ni and NiO can be identified for $(SiO_2)_{90.0}$-$Ni_{10.0}$, implying that most of the nickel species achieves high ionic conductivity and are in the silica framework or highly dispersed on the silica surface. According to previous study [13], high content of Ni^{2+} belonging to type II metal ions act as network intermediates as they become part of the gel network by participating in the condensation polymerization reaction and they are not mobile anymore which makes them not to crystallize out during slow drying of the gel (longer gelation time). Thus, they have low degree of crystallization and strengthen the glass network [13].

BET analysis

BET analysis explains the physical adsorption of gas molecules on a solid surface for the measurement of the specific surface area of materials. Table 1 lists the active surface area of $(SiO_2)_{100-x}$-Ni_x ($x = 2.5$, 10.0). The BET analysis reveals that of $(SiO_2)_{90.0}$-$Ni_{10.0}$ sample has the highest active surface area of 51.6668 $m^2\ g^{-1}$. This is due to the higher amount of Ni dopant in the sample that leads to growth of larger particles and subsequently increases the active surface area of the thin film. In addition, a large active surface area enables more dye and electrolyte to be stored inside the photoanode layer in order for effective photon adsorption to take place resulting in higher PV efficiency [18]. High surface area also promotes greater porosity that may accelerate dye and electrolyte adsorption for smooth electron transport in DSSC mechanism [19].

FESEM analysis

The morphology of the thin films was investigated by FESEM analysis. Figure 5 shows FESEM images of $(SiO_2)_{100-x}$-Ni_x ($x = 2.5$, 10.0) and their corresponding thickness. The annealed thin films show non-uniform spherical particles. The average particle size increased when the dopant amount increased from 2.5 to 10%. The average particle sizes of $(SiO_2)_{97.5}$-$Ni_{2.5}$ and

Table 1 BET analysis of $(SiO_2)_{100-x}$-Ni_x ($x = 2.5$, 10.0)

$(SiO_2)_{100-x}$-Ni_x	Active surface area ($m^2\ g^{-1}$)
$x = 2.5$	00.0383 ± 0.0157
$x = 10.0$	51.6668 ± 0.7810

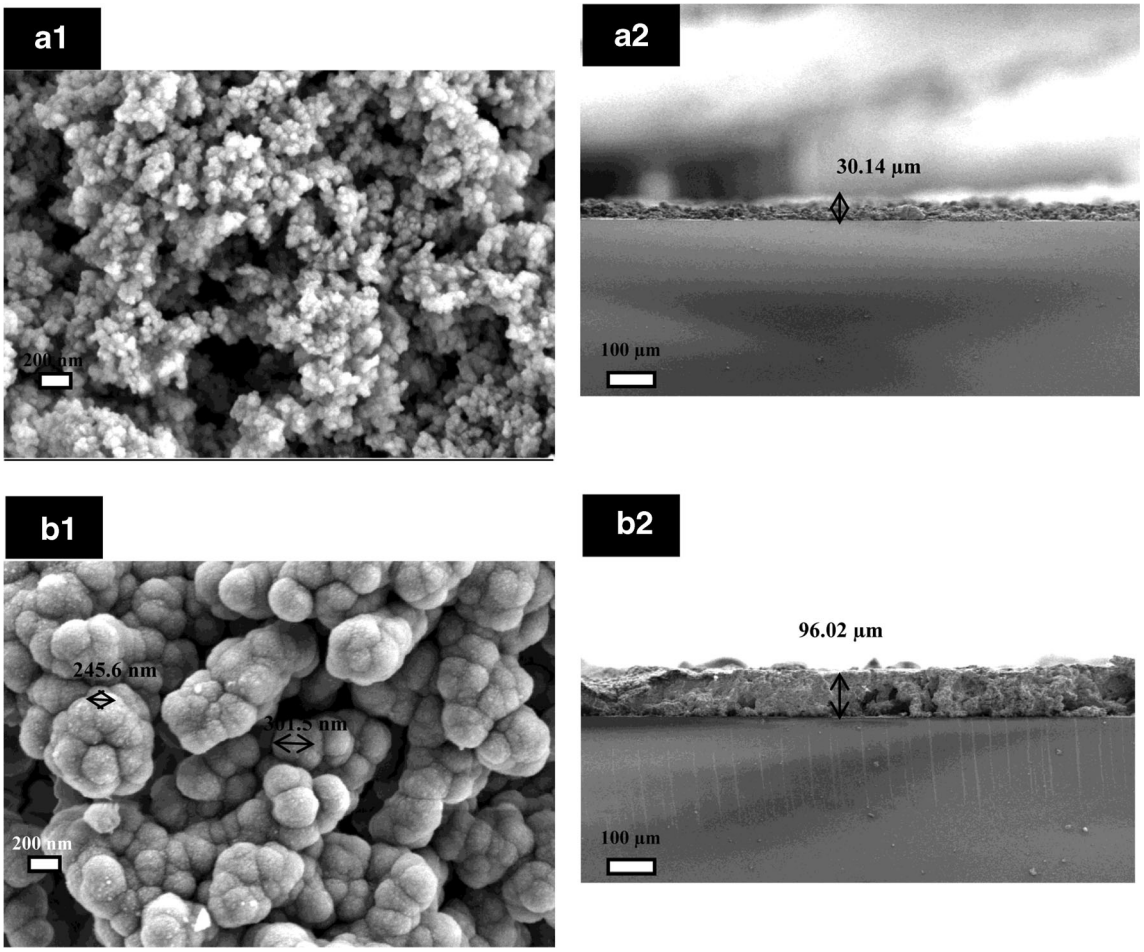

Fig. 5 FESEM images of surface morphology of $(SiO_2)_{100-x}$-Ni_x (a1) $x = 2.5\%$ Ni and (b1) 10.0% Ni and thickness of $(SiO_2)_{100-x}$-Ni_x (a2) $x = 2.5\%$ Ni and (b2) 10.0% Ni

$(SiO_2)_{90.0}$-$Ni_{10.0}$ are 50 nm and 314 nm, respectively. Figure 5 (a1) displays greater porosity as the particles are dense and compact to each other. Greater porosity is also observed in $(SiO_2)_{90.0}$-$Ni_{10.0}$ as observed in Fig. 5 (b1). Larger average particle size in $(SiO_2)_{90.0}$-$Ni_{10.0}$ indicates that increased amount of Ni dopant may attribute to the holding of Ni dopant by SiO_2 matrix. The amorphous SiO_2 traps the Ni^{2+} cations for generating more electrons to facilitate electron transport [17].

Figure 5 (a2) and (b2) show the corresponding thickness of the thin films. The obtained thin films have thickness less than 100 µm. Besides that, thickness of the thin films also plays a crucial role in increasing the performance of the power

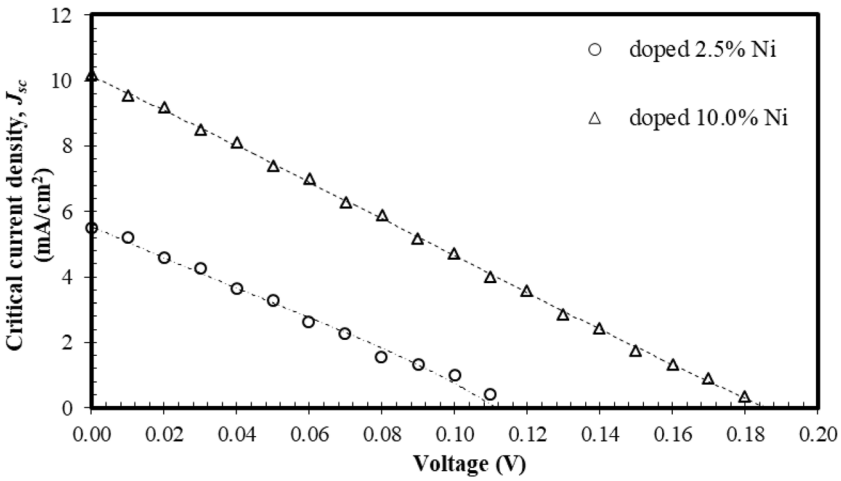

Fig. 6 *J-V* curve of $(SiO_2)_{100-x}$-Ni_x ($x = 2.5$, 10.0) -based dye-sensitized solar cell using liquid electrolyte

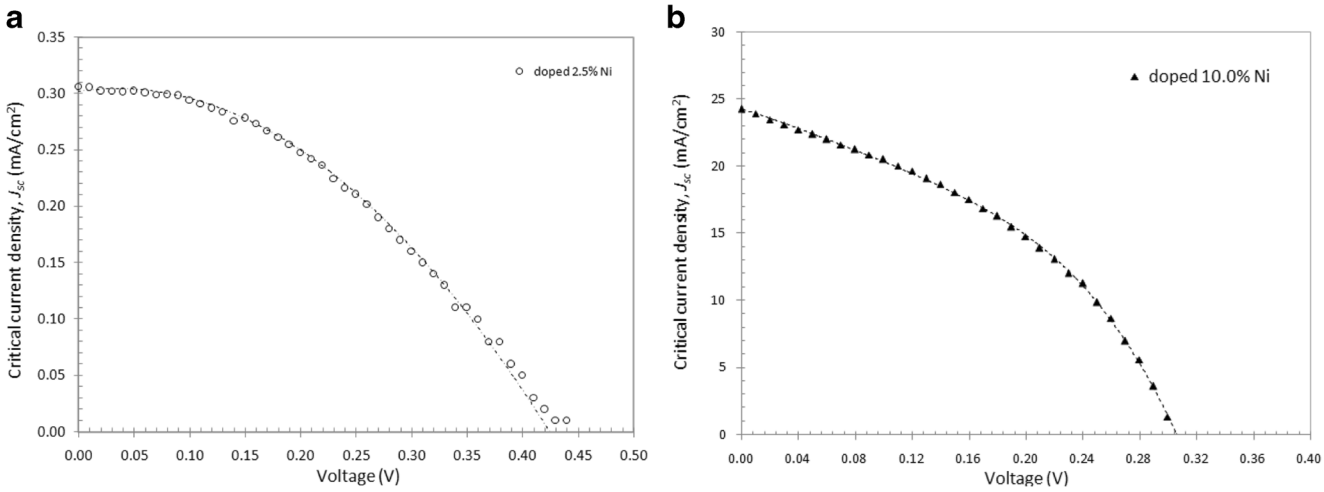

Fig. 7 *J-V* curve of (a) $(SiO_2)_{97.5}$-$Ni_{2.5}$ and (b) $(SiO_2)_{90.0}$-$Ni_{10.0}$ -based dye-sensitized solar cell using PAN-based gel polymer electrolyte

conversion efficiency. The thin films of $(SiO_2)_{90.0}$-$Ni_{10.0}$ shows larger thickness than that of $(SiO_2)_{97.5}$-$Ni_{2.5}$. A thick photoanode allows high dye adsorption rate to ease the electron transport between the excited electron and dye molecule [20].

DSSC photovoltaic performance

Figures 6 and 7 show the *J-V* curve of $(SiO_2)_{100-x}$-Ni_x ($x = 2.5$, 10.0) using liquid electrolyte and PAN-based gel polymer electrolyte, respectively. Table 2 shows the corresponding photovoltaic properties. The solar power conversion efficiency (η) was obtained from the following equations [21],

$$\eta = \frac{V_{oc} \times J_{sc} \times FF}{P_{in}} \quad (1)$$

$$FF = \frac{V_{\max} \times J_{\max}}{V_{oc} \times J_{sc}} \quad (2)$$

where the V_{oc} is the open-circuit voltage obtained at zero current; J_{sc}, the short circuit current that carries the maximum current under less resistance; *FF*, fill factor; V_{max}, the maximum voltage; J_{max}, the maximum current; and P_{in}, intensity of the incident light power.

The result reveals that doping of 10% Ni in SiO_2 and utilization of gel polymer electrolyte increased the power conversion efficiency up to 2.95%. This can be due to the high active surface area, greater porosity, and thicker photoanode observed in BET and FESEM analysis that leads to greater amount of dye adsorption that facilitates electron transport and reduced the electron recombination rate. Besides that, *FF* can be interpreted graphically from the shape of the *J-V* curve. Figure 6 shows a triangular *J-V* curve and Fig. 7 shows a more preferable round-off rectangular shape *J-V* curve where the values of *FF* in Fig. 7 are higher than in Fig. 6. The triangular shape in Fig. 6 interprets poor quality of solar cell.

Moreover, the doping of nickel with gel polymer electrolyte has increased the V_{oc} up to 0.44 V. However, the V_{oc} decreased when the nickel doping was increased from 2.5 to 10%. On the other hand, the J_{sc} showed a sharp increase for higher nickel doping and improved the overall efficiency of DSSC. According to Ahmad et al. [18], nickel doping in SiO_2 may control the bandgap of the SiO_2 and provide a strong absorption to increase DSSC efficiency.

Furthermore, the $(SiO_2)_{97.5}$-$Ni_{2.5}$ thin film with gel polymer electrolyte exhibits higher J_{sc} and lower V_{oc} than that of conventional liquid electrolyte. This result indicates that the KI used in preparation of gel polymer electrolyte assists in increasing the value of V_{oc}. However, the power conversion efficiency of liquid electrolyte was higher than that of gel polymer electrolyte. Hence, the doping of Ni was increased to 10% to overcome this problem. The photoanode of

Table 2 Photovoltaic performance of $(SiO_2)_{100-x}$-Ni_x ($x = 2.5$, 10.0) -based dye sensitized solar cell using liquid electrolyte and PAN-based gel polymer electrolyte

Doping of Nickel (%)	Liquid electrolyte				Gel polymer electrolyte			
	V_{oc} (V)	J_{sc} (mA/cm^2)	*FF*	η (%)	V_{oc} (V)	J_{sc} (mA/cm^2)	*FF*	η (%)
2.5	0.11	5.48	0.27	0.16	0.44	0.31	0.36	0.05
10.0	0.18	10.18	0.26	0.47	0.30	24.31	0.41	2.95

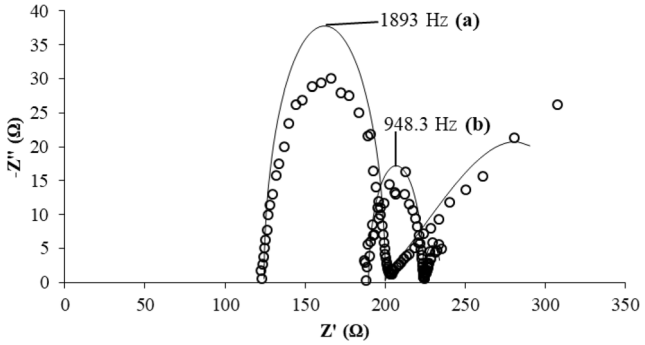

Fig. 8 EIS fitted curves of (a) $(SiO_2)_{97.5}$-$Ni_{2.5}$ and (b) $(SiO_2)_{90.0}$-$Ni_{10.0}$ -based dye-sensitized solar cell using PAN-based liquid electrolyte

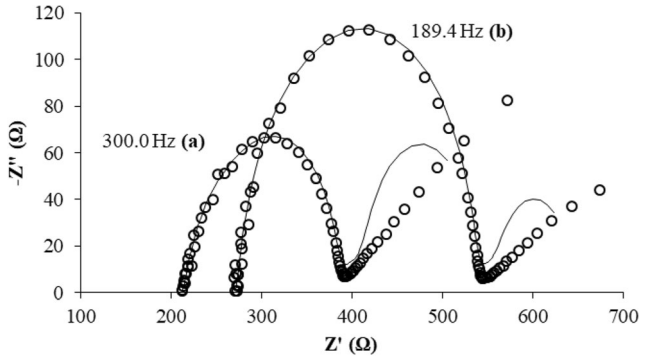

Fig. 9 EIS fitted curves of (a) $(SiO_2)_{97.5}$-$Ni_{2.5}$ and (b) $(SiO_2)_{90.0}$-$Ni_{10.0}$ -based dye-sensitized solar cell using PAN-based gel polymer electrolyte

$(SiO_2)_{90.0}$-$Ni_{10.0}$ using gel polymer electrolyte managed to increase the V_{oc}, J_{sc}, FF, and the overall efficiency of the DSSC. The result shows doping higher amount of Ni in SiO_2 matrix enables to increase the value of J_{sc} from 0.31 to 24.31 mA/cm^2. The result indicates that Ni as dopant can enhance the conductivity in the photoanode layer and may reduce the back transfer electron recombination between the redox electrolyte and the injected electron [22]. Besides that, the high J_{sc} is also due to the high amount of dye adsorption that generates more photogenerated electrons. Mahalingam et al. [23] mentioned that photoanode with large surface area increases the value of J_{sc}.

Electron transport analysis

Figures 8 and 9 show EIS Nyquist plots of $(SiO_2)_{100-x}$-Ni_x ($x = 2.5$, 10.0) using liquid electrolyte and PAN-based gel polymer electrolyte, respectively. EIS analysis is done to investigate the carrier transport in the interface of photoanode/electrolyte. The fitting process was done by referring to a transmission line equivalent circuit as in Fig. 10 [24]. The circuit represents the actual structure of DSSC with resistances and capacitances. The electron transport parameters of EIS include sheet resistance (R_s), substrate resistance (R_{FTO}), transport resistance (R_t), charge transfer resistance (R_{ct}), counter electrode resistance (R_{CE}), Warburg impedance (Z_D), substrate capacitance (C_{FTO}), chemical capacitance (C_μ), and Helmholtz capacitance (C_{CE}).

The electron lifetime (τ_{eff}) and effective rate constant (k_{eff}) are calculated based on previous studies as in the following equations [22]:

$$\tau_{eff} = \frac{1}{2\pi f_{\max}}$$

$$k_{eff} = \frac{1}{\pi_{eff}}$$

where, f_{max} is the maximum frequency of the EIS spectra. The fitted electron transport parameters are listed in Table 3.

According to previous study [25], a large k_{eff} indicates a huge electron recombination rate that causes poor efficiency, and longer electron lifetime denotes that electron

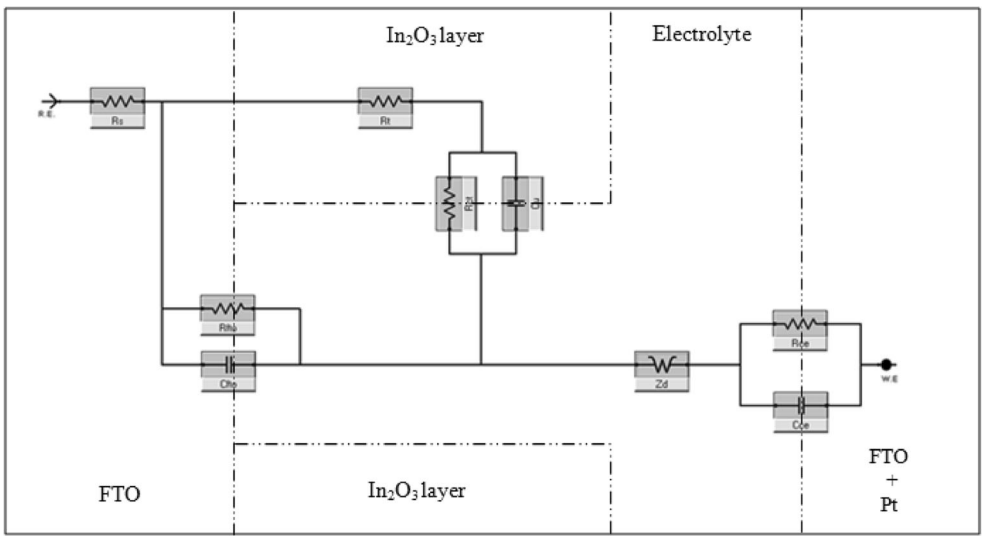

Fig. 10 Equivalent circuit model for EIS data fitting [24]

Table 3 Photovoltaic performance of $(SiO_2)_{100-x}$-Ni_x ($x = 2.5$, 10.0) -based dye sensitized solar cell using liquid electrolyte and PAN-based gel polymer electrolyte

Doping of Nickel (%)	Liquid electrolyte						Gel polymer electrolyte					
	f_{max} (Hz)	R_s (Ω)	R_{ct} (Ω)	R_t (Ω)	τ_{eff} (ms)	k_{eff} (s^{-1})	f_{max} (Hz)	R_s (Ω)	R_{ct} (Ω)	R_t (Ω)	τ_{eff} (ms)	k_{eff} (s^{-1})
2.5	1893	124.3	44,980	150.9	0.08	5959	300	162.4	33.99	85.5	0.53	11,896
10.0	948.3	165.9	380,700	39.43	0.17	1885.2	189.4	270.7	71	169.9	0.84	1190

recombination is prevented effectively at photoanode/electrolyte interface. From Tables 2 and 3.Five percent nickel doping with gel polymer electrolyte has the highest k_{eff} of 11,896 s^{-1} but has greater electron lifetime than nickel doping of 2.5% with liquid electrolyte. Besides that, the electron lifetime for the samples using gel polymer electrolyte is larger compared to that of liquid electrolyte. The result shows that the carrier transport in the interface of photoanode/gel polymer electrolyte gives better sustainability than liquid electrolyte. However, the high electron recombination rate in the sample of 2.5% nickel doping (gel polymer electrolyte) leads to a very low J_{sc} (0.31 mA/cm^2) that caused the overall power conversion efficiency to decrease tremendously.

The J_{sc} was able to increase after doping 10% of nickel in the samples of both liquid and gel polymer electrolyte. The samples exhibited slow electron recombination rate than 2.5% nickel doping. The result shows that the transition metal (nickel) has the ability to increase the J_{sc} by controlling the bandgap of SiO_2 and providing strong absorption to increase DSSC efficiency [18]. Furthermore, by comparing between liquid and gel polymer electrolyte, the samples doped with 10% of nickel with gel polymer electrolyte gives longer electron lifetime (0.84 ms) and smaller recombination rate (1190 s^{-1}). This result indicates that gel polymer electrolyte provides greater sustainability with optimum amount of nickel doping of 10% facilitates the electron transport in the cell and leads to improved power conversion efficiency.

Conclusion

In summary, $(SiO_2)_{100-x}$-Ni_x ($x = 2.5$, 10.0) was successfully prepared by using novel sol-gel method. The utilization of PAN-based gel polymer electrolyte in the higher amount of Ni (10%) dopant in SiO_2 photoanode-based DSSC significantly increased the power conversion efficiency up to 2.96%. The XRD patterns revealed that $(SiO_2)_{90.0}$-$Ni_{10.0}$ thin film is more capable of holding the Ni^{2+} ion in SiO_2 matrix by generating more electrons to facilitate the electron transport in the DSSCs. The FESEM images show larger average particle size with greater porosity in the $(SiO_2)_{90.0}$-$Ni_{10.0}$ thin film. In addition, the FESEM image also shows that the $(SiO_2)_{90.0}$-$Ni_{10.0}$ thin film is thicker and may allow high dye adsorption rate between the excited electron and dye molecule. Meanwhile, the BET analysis determines greater active surface area on $(SiO_2)_{90.0}$-$Ni_{10.0}$ thin films that indicate more dye molecules may adsorb on the mesoporous photoanode to facilitate electron transport in the DSSC. The higher amount of Ni doping (10%) in SiO_2 exhibits significantly greater value of short-circuit current density (J_{sc}) of 24.31 mA/cm^2 indicating high ionic conductivity that reduces the electron recombination rate between the redox electrolyte and the injected electron in the DSSC mechanism. Moreover, the utilization of PAN-based gel polymer electrolyte improved the value of open-circuit voltage (V_{oc}) due to its greater ionic conductivity and mechanical stability compared to that of liquid electrolyte in the DSSC.

Acknowledgments This work was supported by Project No.: UKM-DIP-2016-021and Photonic Technology Laboratory (IMEN), Department of Electrical, Electronic and Systems Engineering, Universiti Kebangsaan Malaysia, Bangi, Selangor, Malaysia.

References

1. Ciani L, Catelani M, Carnevale EA, Donati L, Bruzzi M (2015) Evaluation of the aging process of dye sensitized solar cell under different stress conditions. IEEE Trans Instrum Meas 64:1179–1187
2. Mahalingam S, Abdullah H (2016) Electron transport study of indium oxide as photoanode in DSSCs: a review. Renew Sustain Energy Rev 63:245–255
3. O'Regan B, Grätzel M (1991) A low-cost, high-efficiency solar cell based on dye-sensitized colloidal TiO_2 films. Nature 353:737–740
4. Mahalingam S, Abdullah H, Shaari S, Muchtar A (2016) Improved catalytic activity of Pt/rGO counter electrode in In_2O_3-based DSSC. Ionics 22:2487–2497
5. Mahalingam S, Abdullah H, Ashaari I, Shaari S, Muchtar A (2016) Influence of heat treatment process in In_2O_3-MWCNTs as photoanode in DSSCs. Ionics 22:711–719
6. Bisquert J (2002) Theory of the impedance of electron diffusion and recombination in a thin layer. J Phys Chem B 106:325–333
7. Abdullah H, Atiqah NA, Omar A, Asshaari I, Mahalingam S, Razali Z, Shaari S, Mandeep JS, Misran H (2015) Structural, morphological, electrical and electron transport studies in ZnO–rGO (wt%= 0.01, 0.05 and 0.1) based dye-sensitized solar cell. J Mater Sci Mater Electron 26:2263–2270

8. Mahalingam S, Abdullah H, Omar A, Nawi NAM, Shaari S, Muchtar A, Asshari I (2015) Effect of morphology on SnO_2/MWCNT-based DSSC performance with various annealing temperatures. Adv Mater Res 1107:649
9. Mahalingam S, Abdullah H, Ashaari I, Shaari S, Muchtar A (2016) Optical, morphology and electrical properties of In_2O_3 incorporating acid-treated single-walled carbon nanotubes based DSSC. J Phys D Appl Phys 49:075601
10. Son S, Hwang SH, Kim C, Yun JY, Jang J (2013) Designed synthesis of SiO_2/TiO_2 core/shell structure as light scattering material for highly efficient dye-sensitized solar cells. ACS Appl Mater Interfaces 5:4815–4820
11. Shin YJ, Lee JH, Park JH, Park NG (2007) Enhanced photovoltaic properties of SiO_2-treated ZnO nanocrystalline electrode for dye-sensitized solar cell. Chem Lett 36:1506–1507
12. Li GR, Song J, Pan GL, Gao XP (2011) Highly Pt-like electrocatalytic activity of transition metal nitrides for dye-sensitized solar cells. Energy Environ Sci 4:1680–1683
13. Yang CH, Ho WY, Yang HH, Hsueh ML (2010) Approaches to gel electrolytes in dye-sensitized solar cells using pyridinium molten salts. J Mater Chem 20(29):6080–6085
14. Dissanayake MA, Bandara LR, Bokalawala RS, Jayathilaka PA, Ileperuma OA, Somasundaram S (2002) A novel gel polymer electrolyte based on polyacrylonitrile (PAN) and its application in a solar cell. Mater Res Bull 37:867–874
15. Arof AK, Aziz MF, Noor MM, Careem MA, Bandara LR, Thotawatthage CA, Rupasinghe WN, Dissanayake MA (2014) Efficiency enhancement by mixed cation effect in dye-sensitized solar cells with a PVdF based gel polymer electrolyte. Int J Hydrog Energy 39:2929–2935
16. Careem MA, Aziz MF, Buraidah MH (2017) Boosting efficiencies of gel polymer electrolyte based dye sensitized solar cells using mixed cations. Mater Today: Proc 4(4):5092–5099
17. Bandara TMWJ, Jayasundara WJMJSR, Dissanayake MAKL, Furlani M, Albinsson I, Mellander BE (2013) Effect of cation size on the performance of dye sensitized nanocrystalline TiO2 solar cells based on quasi-solid state PAN electrolytes containing quaternary ammonium iodides. Electrochim Acta 109:609–616
18. Ahmad M, Abdullah H, Yuliarto B (2018) Effect of nickel in TiO 2-SiO 2-GO-based DSSC by using a sol-gel method. Ionics 6:1
19. Mathew S, Yella A, Gao P, Humphry-Baker R, Curchod BF, Ashari-Astani N et al (2014) Dye-sensitized solar cells with 13% efficiency achieved through the molecular engineering of porphyrin sensitizers. Nat Chem 6:242–247
20. Mahalingam S, Abdullah H, Razali MZ, Yarmo MA, Shaari S, Omar A (2016) Structural, morphological, photovoltaic and electron transport properties of ZnO based DSSC with different concentrations of MWCNTs. Mater Sci Forum 846:2016
21. Wen P, Han Y, Zhao W (2012) Influence of TiO_2 nanocrystals fabricating dye-sensitized solar cell on the absorping spectra of N719 sensitizer. Int J Photoenergy 2012. https://doi.org/10.1155/2012/906198
22. Bisquert J, Zaban A, Greenshtein M, Seró IM (2004) Determination of rate constants for charge transfer and distribution of semiconductor and electrolyte electronic energy levels in dye-sensitized solar cells by open-circuit photovoltage decay method. J Am Chem Soc 126:13550–13559
23. Mahalingam S, Abdullah H, Shaari S, Muchtar A (2016) Morphological and electron mobility studies in nanograss In_2O_3 DSSC incorporating multi-walled carbon nanotubes. Ionics 22:1985–1997
24. Mahalingam S, Abdullah H, Manap A (2018) Role of acid-treated CNTs in chemical and electrochemical impedance study of dye-sensitised solar cell. Electrochim Acta 264:275–283
25. Mahalingam S, Abdullah H, Amin N, Manap A Incident photon-to-current efficiency of thermally treated SWCNTs-based nanocomposite for dye-sensitized solar cell. Ionics 1–5. https://doi.org/10.1007/s11581-018-2629-9